# Energy-Aware Flexible Flow Shop Scheduling with Solar PV, Battery Storage, and Demand Response: A Genetic Algorithm Approach

Joyce MHANNA[1,2], Hajar NOUINOU[1], Simon CAILLARD[3] and David BAUDRY[4]

*Abstract*— **Green manufacturing increasingly requires production systems to balance operational performance with energy efficiency and cost-effectiveness. This paper addresses an energy-aware flexible flow shop scheduling problem in which a factory operates under a time-of-use electricity tariff, participates in a demand response reward program, exploits on-site photovoltaic generation, battery energy storage, and applies an on/off machine strategy to reduce idle power consumption. Two objectives are optimized in lexicographic order: makespan as the primary criterion and net energy cost, electricity expenditure minus demand response rewards collected, as the secondary one. A Genetic Algorithm is proposed, combining an order-crossover permutation encoding, an earliest-finish-time decoder, and an energy management heuristic. Results show that the approach produces compact, energy-efficient schedules, while a sensitivity analysis highlights the strong impact of demand response incentives on reducing net energy costs without affecting production throughput.**

## I. Introduction

The industrial sector is responsible for approximately 37% of global energy consumption [1], yet in many countries renewable sources still account for a small fraction of that total. Against the backdrop of Industry 5.0, which places sustainability at the heart of manufacturing [2], integrating energy criteria into production planning has become a pressing challenge. Industrial facilities increasingly combine on-site photovoltaic (PV) generation with Battery Energy Storage Systems (BESS) to reduce their dependence on the grid, while electricity network operators deploy Demand Side Management (DSM) strategies, including Time-Of-Use (TOU) tariffs and Demand Response (DR) incentive programs, to smooth consumption peaks [3], [4]. Scheduling decisions determine when and how much power is consumed by production equipment; they therefore constitute a key lever for reducing energy costs while preserving operational performance.

Energy-aware scheduling has attracted sustained research attention over the past two decades, with contributions organized around two complementary axes: Energy Efficiency (EE) and Energy Flexibility (EF).

EE strategies aim to reduce the power consumed during production without degrading throughput. The most studied approach is Variable Machine Speed (VMS), where processing time and power draw are coupled through a speed variable. Mansouri et al. [5] studied the makespan-energy trade-off in a two-machine flow shop with sequence-dependent setup times, proposing a multi-objective MILP solved via $\epsilon$-constraint. Öztop et al. [6] extended this to a Flexible Flow Shop (FFS) and benchmarked seven bi-objective metaheuristics against MILP and Constraint Programming (CP) models. Wei et al. [7] addressed a flexible job shop with VMS and an NSGA-II approach to jointly minimize makespan and total energy consumption. A complementary EE lever is the on/off machine strategy, which switches machines off during inter-job gaps when idling cost exceeds the restart cost. Mouzon et al. [8] pioneered this approach on a single machine, demonstrating that significant energy savings are achievable by powering down under-utilised equipment. Ham et al. [9] extended it to a flexible job shop, comparing MILP and CP formulations. Shrouf et al. [10] combined on/off switching with TOU pricing on a single machine and proposed a genetic algorithm, providing an early bridge between EE and EF.

Energy flexibility strategies shift or curtail load in response to electricity price signals or DR programs. TOU pricing is the most widely studied mechanism, as it closely mirrors real industrial contracts and is straightforward to integrate into scheduling models [4]. Ho et al. [11] derived optimality conditions for a two-machine permutation flow shop under TOU and proposed a Benders-decomposition MILP. Zhang et al. [12] minimized $CO_2$ emissions and Total Electricity Cost (TEC) simultaneously in a flow shop under TOU with on/off machines. Park and Ham [13] addressed makespan and TEC minimization in a flexible job shop under TOU, comparing MILP and CP on benchmark instances of varying sizes. Biel et al. [14] incorporated stochastic wind generation into a flow shop and used a two-stage stochastic program to jointly minimize weighted completion times and TEC. Several works additionally integrate on-site renewables and storage. Zhang et al. [15] considered a grid-connected FFS factory with on-site PV and BESS, minimizing TEC while accounting for buffer constraints and machine maintenance. Moon and Park [16] combined renewable sources, BESS, and TOU pricing in a flexible job shop, minimizing total production cost including overtime penalties linked to the makespan. Subramanyam et al. [17] used two-stage stochastic programming to jointly size renewables and BESS for a FFS factory subject to annual throughput requirements.

Combined EE and EF approaches are comparatively rarer but increasingly recognized as essential for realistic industrial models. Luo et al. [18] jointly optimized TOU electricity cost

[1] CESI LINEACT, 54000 Nancy, France
[2] Agence de l'environnement et de la Maîtrise de l'Energie, 49004 Angers, France
[3] CESI LINEACT, 51100 Reims, France
[4] CESI LINEACT, 76800 Rouen, France
{jmhanna, hnouinou, scaillard, dbaudry}@cesi.fr

and machine efficiency via VMS in a FFS, proposing an ant colony metaheuristic. Schulz et al. [19] minimized total tardiness and TEC in a FFS with VMS and TOU, comparing time-indexed and sequence-based MILP formulations. Zhai et al. [20] combined on-site wind generation, real-time pricing, and on/off switching in a flow shop MILP.

Despite this growing body of work, no existing study simultaneously integrates TOU pricing, a DR demand-bidding reward program, on-site PV generation, BESS, and an on/off machine strategy within a FFS environment. Furthermore, most studies developed exact methods, which are limited to small instances, while existing metaheuristics do not jointly manage the full energy system but rather focus on scheduling optimization alone including an EE strategy.

This paper addresses a FFS machine environment where jobs are processed sequentially through multiple stages each equipped with parallel machines. Two objectives are optimized in lexicographic order: makespan as the primary criterion and net energy cost as the secondary one, ensuring that production throughput remains the foremost priority for factory operations. The main contributions of this work are:

- An energy-aware FFS problem integrating TOU pricing, a DR reward program, on-site PV, a BESS, and an on/off machine strategy.
- A GA with an embedded energy management heuristic that jointly coordinates scheduling, battery operation, and DR participation.
- A sensitivity analysis assessing the impact of key energy and operational parameters on schedule performance and net energy cost.

The remainder of this paper is organized as follows. Section II formally describes the problem. Section III presents the proposed GA and energy management heuristic. Section IV illustrates the approach on a representative instance, and Section V reports a sensitivity analysis on the key energy-market parameters. Finally, Section VI concludes and outlines future work.

## II. Problem Description

### A. Production System

We consider an energy-aware FFS scheduling problem. The process consists of $n_s$ sequential production stages, indexed by $\mathcal{S} = \{1, 2, \dots, n_s\}$. Each stage $s \in \mathcal{S}$ contains $m_s \geq 1$ parallel machines, so the total number of machines is $M = \sum_{s=1}^{n_s} m_s$. A set of $N$ independent jobs $\mathcal{J} = \{1, \dots, N\}$ must each be processed through all the stages in the same order. Each job visits exactly one machine per stage, the machine is selected at scheduling time. Once started, an operation cannot be interrupted (no preemption). A job may not begin its operation at stage $s+1$ before it has completed stage $s$ (precedence constraint), and each machine can process at most one job at a time (capacity constraint).

Table I summarizes the main symbols used throughout the paper.

TABLE I

NOTATION SUMMARY

| Symbol | Definition | Acronym | Definition |
|---|---|---|---|
| $n_s$, $N$, $M$ | Number of stages, jobs, machines | PV | Photovoltaic |
| $\mathcal{S}$,$\mathcal{J}$,$\mathcal{M}_s$ | Set of jobs; set of stages; set of machines at stage $s$ | BESS | Battery Energy Storage Systems |
| $m_s$ | Number of parallel machines at stage $s$ | DSM | Demand Side Management |
| $p_{j,k,s}$ | Processing time of job $j$ on machine $k$ at stage $s$ | TOU | Time-Of-Use |
| $e_{j,k,s}$ | Active power of job $j$ on machine $k$ at stage $s$ (kW) | DR | Demand Response |
| $p^{\text{idle}}_{k,s}$ | Idle power of machine $k$ at stage $s$ (kW) | EE | Energy Efficiency |
| $p^{\text{on}}_{k,s}$ | Turn-on power for machine $k$ at stage $s$ (kW) | EF | Energy Flexibility |
| $\tau^{\text{on}}_{j,k,s}$ | Turn-on duration for job $j$ on machine $k$ at stage $s$ | VMS | Variable Machine Speed |
| $T_f$ | Length of scheduling horizon (slots) | FFS | Flexbile Flow Shop |
| $\text{PV}_t$ | PV generation at slot $t$ (kW) | MILP | Mixed-Integer Linear Programming |
| $C_b$, $L_c$, $L_d$ | Battery capacity, charge/discharge limits (kW) | CP | Constraint Programming |
| $\eta_c$, $\eta_d$ | Charging / discharging efficiency | TEC | Total Electricity Cost |
| $\lambda_t$ | Electricity tariff at slot $t$ (\$/kWh) | GA | Genetic Algorithm |
| $\overline{C}_t$ | DR contractual baseline at slot $t$ (kW) | EFT | Earliest Finish Time |
| $\overline{LR}$ | Minimum load reduction for DR reward (kW) | | |
| $\rho_t$ | DR reward rate at slot $t$ (\$/kWh) | | |
| $P^G_t$, $P^C_t$, $P^D_t$ | Grid, charge, discharge power at slot $t$ | | |
| $C_{\max}$, $f_2$ | Makespan; net energy cost | | |

### B. Machine Energy States

Beyond processing, each machine operates in one of three energy states at any time slot, each carrying a distinct power draw:

- **Processing**: while executing job $j$, machine $k$ at stage $s$ consumes a job-dependent active power $e_{j,k,s}$ (kW).
- **Idle**: when machine $k$ at stage $s$ stays on between consecutive jobs, it consumes standby power $p^{\text{idle}}_{k,s}$.
- **Turn-on**: if a machine $k$ at stage $s$ is switched off between jobs, it requires a warm-up phase of duration $\tau^{\text{on}}_{j,k,s}$ at power $p^{\text{on}}_{k,s}$ before the next job $j$ can start. The controller selects between idling and turning off by comparing the two energy costs over the gap between consecutive operations.

The aggregate power demand $d_t$ of the factory at each time slot $t$ is the sum of all active, idle, and turn-on powers across all machines.

### C. On-Site Energy System

The factory is equipped with an on-site energy system composed of three elements:

- **Photovoltaic (PV)**: delivers a time-varying generation profile $\text{PV}_t$ (kW) over the scheduling horizon. PV energy is used to cover machine demand first, before any grid or battery resource is solicited.
- **Battery energy storage**: a storage unit of capacity $C_b$ (kWh) with a maximum charge rate $L_c$ and discharge rate $L_d$ (both in kW), and round-trip efficiencies $\eta_c$ (charging) and $\eta_d$ (discharging). The battery absorbs PV surplus or off-peak grid energy, and releases it during high-tariff periods.
- **Grid connection**: the factory can import electricity from the grid at any time. The electricity tariff $\lambda_t$ follows a TOU structure with three price levels: off-peak, mid-peak, and on-peak. Grid power drawn at slot $t$ is denoted $P^G_t$ (kW).

### D. Demand Response Incentive

The factory participates in a DR program. At each time slot $t$ in which a reward signal $\rho_t > 0$ is broadcast, the factory receives a financial reward if its grid consumption $P^G_t$

falls below a contractual baseline $\overline{C}_t$ by at least a threshold $\overline{LR}$ (kW). The reward collected at slot $t$ is:

$$R_t = \begin{cases} \left(\overline{C}_t - P_t^G\right)\rho_t & \text{if } \rho_t > 0 \text{ and } \overline{C}_t - P_t^G \geq \overline{LR}, \\ 0 & \text{otherwise.} \end{cases} \tag{1}$$

This mechanism incentivizes the factory to shift flexible loads (machine operations, battery charging) away from peak demand events.

### E. Objectives and Optimization Criterion

The problem involves two objectives:

- $f_1$ - **Makespan**: $C_{\max} = \max_{j \in \mathcal{J}} C_j$, where $C_j$ is the completion time of job $j$ at stage $n_s$. Minimizing $C_{\max}$ reflects the production throughput requirement.
- $f_2$ - **Net energy cost**: $f_2 = \sum_t \left(\lambda_t P_t^G - R_t\right)$. Minimizing $f_2$ captures both electricity bill reduction and DR reward maximization.

The two objectives are optimized in *lexicographic* order: production efficiency (makespan) takes strict priority over energy cost. A solution $\mathbf{a}$ is considered better than $\mathbf{b}$ if $f_1(\mathbf{a}) < f_1(\mathbf{b})$, or if $f_1(\mathbf{a}) = f_1(\mathbf{b})$ and $f_2(\mathbf{a}) < f_2(\mathbf{b})$. This ordering reflects an industrial context where delivery deadlines are non-negotiable, and energy savings are pursued only when they do not jeopardize throughput.

## III. Proposed Methodology

### A. Solution Representation and Decoding

A solution is encoded as a *permutation* $\pi = (\pi_1, \pi_2, \ldots, \pi_N)$ of the $N$ job indices, shared across all stages. Given $\pi$, the schedule is built by a *greedy earliest-finish-time* (EFT) decoder that processes jobs in the order prescribed by $\pi$ at each stage independently. For each job $j = \pi_i$ at stage $s$, the decoder selects the eligible machine $k^*$ that minimizes the job's completion time:

$$k^* = \arg\min_{k \in \mathcal{M}_s} \Big(\max\big(r_j,\, a_k\big) + p_{j,k,s}\Big), \tag{2}$$

where $r_j$ is the earliest availability time of job $j$ (equal to its completion time at stage $s-1$), and $a_k$ is the time at which machine $k$ becomes available. If no eligible machine exists for a given job, the solution is deemed infeasible.

### B. Energy Management Heuristic

Once the schedule is fixed, the gross power demand $d_t$ (kW) at each time slot $t$ is computed by aggregating the processing, idle, and turn-on powers of all machines according to their assigned intervals. Between two consecutive jobs on the same machine, the controller compares the cost of keeping the machine idle (power $p^{\text{idle}}$) versus switching it off and paying the turn-on cost for the next job; the cheaper option is selected.

Available PV generation is applied first: the *net demand* forwarded to the battery/grid layer is $d_t^{\text{net}} = \max(0, d_t - \mathrm{PV}_t)$. The battery is then managed by a rule-based heuristic (*charge_discharge*) that partitions the active horizon $[0, \lceil C_{\max} \rceil]$ into time periods derived from the TOU tariff structure:

- *Off-peak* ($\lambda_t = \lambda_{\min}$): charge the battery from the grid up to the amount needed to serve upcoming peak demand, using any PV surplus first.
- *Peak* ($\lambda_t = \lambda_{\max}$): discharge the battery to reduce grid imports, subject to limits $L_d$ and $\eta_d$.
- *Mid-peak* periods: cautious discharge before the second peak block; PV surplus is stored whenever possible.

At each slot $t$, the battery state of charge $B_t$, charging power $P_t^C$, discharging power $P_t^D$, and grid power $P_t^G$ satisfy:

$$B_t = B_{t-1} + P_t^C - P_t^D, \tag{3}$$

$$0 \leq P_t^C \leq L_c, \quad 0 \leq B_t \leq C_b, \tag{4}$$

$$P_t^G = \max\Big(0,\, d_t^{\text{net}} + \tfrac{P_t^C}{\eta_c} - \eta_d P_t^D\Big). \tag{5}$$

After computing $P_t^G$ for all time slots, the net cost $f_2$ is evaluated accounting for DR rewards (see Section II). All variables are set to zero beyond the active horizon $\lceil C_{\max} \rceil$ to avoid spurious costs from unoccupied time slots.

### C. Genetic Algorithm

The GA operates on a population of $|\mathcal{P}|$ permutation chromosomes. Each chromosome is evaluated by the EFT decoder followed by the energy management heuristic, yielding a fitness tuple $(f_1, f_2)$. Chromosomes are compared using the lexicographic dominance relation defined in Section II.

*Initialization:* The initial population is generated by drawing $|\mathcal{P}|$ independent uniform random permutations of $\{1, \ldots, N\}$.

*Selection:* Binary tournament selection is used: two chromosomes are drawn uniformly at random from the current population and the lexicographically better one is retained as a parent.

*Crossover:* Order Crossover (OX) is applied with probability $p_c$. Given parents $\pi^{(1)}$ and $\pi^{(2)}$, two cut points $[s, e)$ are chosen at random; the segment $\pi^{(1)}[s:e]$ is copied into the child, and the remaining positions are filled in the relative order they appear in $\pi^{(2)}$, skipping already-present jobs. If no crossover occurs (probability $1 - p_c$), the first parent is cloned.

*Mutation:* A swap mutation is applied with probability $p_m$: two distinct positions $i_1$ and $i_2$ are chosen uniformly at random and their values are exchanged.

*Replacement:* Elitist generational replacement is used: the best solution found so far is carried over to the next generation without modification, and the remainder of the new population is filled by the offspring described above.

The complete procedure is summarized in Algorithm 1.

### D. Parameter Settings

The main parameters of the GA are as follows: the population size $|\mathcal{P}| = 100$, the number of generations $G = 150$, the crossover probability $p_c = 0.6$ and the mutation probability $p_m = 0.05$.

**Algorithm 1** Genetic Algorithm for Energy-Aware FFS

**Input:** instance data, $|\mathcal{P}|$, $G$, $p_c$, $p_m$
Initialize population $\mathcal{P}$ with $|\mathcal{P}|$ random permutations
$\pi^* \leftarrow \arg\min_{\pi \in \mathcal{P}} (f_1(\pi), f_2(\pi))$
**for** $g = 1$ to $G$ **do**
  Evaluate $(f_1(\pi), f_2(\pi))$ for all $\pi \in \mathcal{P}$
  Update $\pi^*$ if a better solution is found
  $\mathcal{P}' \leftarrow \{\pi^*\}$ (elitism)
  **while** $|\mathcal{P}'| < |\mathcal{P}|$ **do**
    $\pi^{(1)} \leftarrow$ TOURNAMENT($\mathcal{P}$)
    $\pi^{(2)} \leftarrow$ TOURNAMENT($\mathcal{P}$)
    **if** Uniform$(0,1) < p_c$ **then**
      $\pi_{\text{child}} \leftarrow$ OX-CROSSOVER($\pi^{(1)}, \pi^{(2)}$)
    **else**
      $\pi_{\text{child}} \leftarrow \pi^{(1)}$
    **end if**
    **if** Uniform$(0,1) < p_m$ **then**
      SWAPMUTATION($\pi_{\text{child}}$)
    **end if**
    $\mathcal{P}' \leftarrow \mathcal{P}' \cup \{\pi_{\text{child}}\}$
  **end while**
  $\mathcal{P} \leftarrow \mathcal{P}'$
**end for**
**return** $\pi^*$

## IV. Illustrative Example

### A. Instance Description

To illustrate the behaviour of the proposed approach, we consider an instance with the following configuration : three stages where the first and third stages include three parallel machines while the second stage includes two machines, a total of $M = 8$ machines and $N = 10$ jobs. The scheduling horizon spans $T_f = 197$ time slots. Table II summarizes the key parameters of this instance.

TABLE II
ILLUSTRATIVE INSTANCE CONFIGURATION

| Parameter | Value | Parameter | Value |
|---|---|---|---|
| Battery cap. $C_b$ (kWh) | 100 | TOU structure | Off/On-peak |
| Max charge rate $L_c$ (kW) | 50 | Off-peak tariff $\lambda_{\min}$ | 0.0101 |
| Max discharge rate $L_d$ (kW) | 50 | On-peak tariff $\lambda_{\max}$ | 0.0223 |
| Charge eff. $\eta_c$ | 0.95 | TOU ratio $r$ | 2.2× |
| Discharge eff. $\eta_d$ | 0.95 | DR baseline $\overline{C}_t$ (kW) | 119 |

The TOU tariff follows a two-level structure: an off-peak rate of 0.0101 \$/kWh, while an on-peak rate of 0.0223 \$/kWh (approximately 2.2× higher). With 10 jobs and only 2 machines at stage 2, the schedule is expected to extend well into the peak window, making the battery pre-charging strategy particularly relevant. A PV generation profile is available throughout the horizon, with modest solar output that partially offsets machine demand during mid-horizon slots.

### B. Obtained Schedule and Energy Profile

The GA (population size 100, 150 generations, 5 independent runs) produces a best solution with a makespan of 55 time slots and a net energy cost of 3.7\$. Figs. 1 and 2 show the resulting Gantt chart and energy profile respectively. This solution matches the optimal makespan obtained using the MILP approach [21], while a gap of 4.15 \$ remains on the TECR objective.

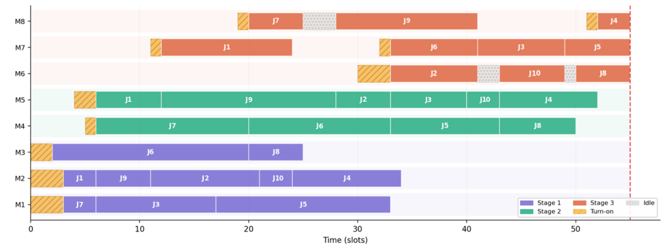


Fig. 1. Gantt chart for the illustrative example instance

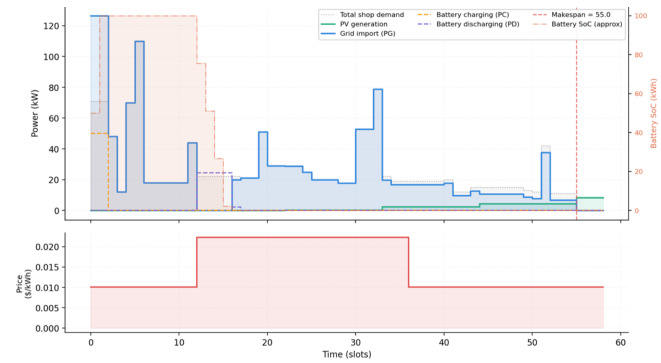


Fig. 2. Energy profile for the illustrative example instance

The Gantt chart reveals that all 10 jobs are dispatched immediately to the three stage-1 machines (M1-M3), with brief turn-on phases at the very start of the horizon. Stage 2 (M4-M5) is the binding bottleneck: with only 2 machines serving 10 jobs, both machines operate continuously with no idle gaps, and several jobs must queue before they can proceed. This queuing effect extends the active horizon to slot 55, well beyond the peak tariff window (slots 12-35), and drives the bulk of energy demand into the high-price period. At stage 3 (M6-M8), jobs are released as they complete stage 2, spreading completion times toward the end of the planning horizon. The last job to finish determines the makespan.

Regarding the energy profile, the factory demand peaks sharply during the first few slots as all 10 jobs simultaneously enter stage 1, then decreases progressively as jobs complete at different rates. The algorithm pre-charges the battery during the off-peak window (slots 0-11) using cheap grid energy ($P_t^C \approx 50$ kW), building a state of charge that is subsequently discharged during the peak window (slots 12-35) to reduce grid imports. With 10 jobs active during the peak period, the battery discharge alone cannot cover the full demand, so a residual grid import at peak rate unavoidably remains. PV generation contributes modestly throughout, partially offsetting machine demand during mid-horizon slots when jobs are still being processed at stages 2 and 3. Overall, the algorithm successfully shifts the cost burden from peak to off-peak slots, directly lowering $f_2$.

The GA was evaluated on large-scale instances of 15, 20, and 30 jobs to analyze its robustness and stability. The variation between the minimum, average, and maximum makespan values remains small, with an average gap of about 3 % for 15 jobs and nearly 4 % for 20 and 30 jobs, indicating good stability despite the increasing problem size. Meanwhile, the average execution time grows with instance complexity, from about 24s for 15 jobs to 39s for 30 jobs.

## V. Sensitivity Analysis

### A. Experimental Design

To assess the robustness of the proposed approach with respect to energy-market parameters and machine operating conditions, we perform three sensitivity experiments that directly affect the trade-off between scheduling efficiency and energy cost:

a. **TOU price ratio** $r = \lambda_{\max}/\lambda_{\min}$: varying from $1.5\times$ to $5.0\times$ (six levels). A higher ratio increases the financial incentive to shift load away from peak slots.
b. **DR reward scale** $\alpha$: a multiplier applied to the base reward vector $\rho_t$, varying from 0 (no DR program) to $3\times$ (six levels), where the contractual baseline is set to realistic values matching the illustrative example's data and the reward levels reflect personalized load-reduction profiles across industrial consumers [22].
c. **Machine power mode** $\mu = (p_t, p_e)$: a discrete operating-mode parameter that jointly scales the per-job processing time by a factor $p_t$ and the per-machine energy consumption by a factor $p_e$, spanning six levels from (1.5, 0.5) to (0.6, 1.8). The pair (1.0, 1.0) corresponds to the baseline instance, while lower values of $p_t$ (and correspondingly higher values of $p_e$) reflect faster, more energy-intensive operation, and higher values of $p_t$ (with lower $p_e$) reflect slower, more energy-efficient operation.

The first two dimensions are evaluated jointly over a $6 \times 6 = 36$ parameter grid (Experiments a and b), while the Experiment c varies $\mu$ independently with all other parameters fixed at their baseline values. For every configuration, the GA is run 5 times independently and the best solution is retained, yielding 180 executions for the joint grid and 30 additional executions for the power-mode experiment, for a total of 210 GA runs. The same lexicographic objective (makespan first, then net energy cost) is enforced throughout all experiments.

### B. Results and Discussion

Figure 3 presents a joint view of both objectives over the full $6 \times 6$ grid (Experiments a and b), while Figure 4 illustrates the effect of the power mode $\mu = (p_t, p_e)$ on makespan and net energy cost (Experiment c).

The following findings emerge from the results:

**Exp-a. TOU price ratio effect on energy cost.** In the absence of DR ($\alpha = 0$), the net cost increases slightly with the TOU ratio (from 1.7 at $r = 1.5$ to 4.5 at $r = 5.0$). Although a higher peak price should motivate greater battery utilisation and therefore lower costs, the battery capacity and discharge rate ($C_b = 100$ kWh, $L_d = 50$ kW) are insufficient to fully cover the peak-period demand of 10

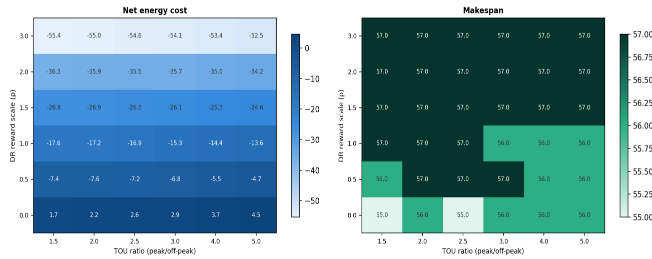


Fig. 3. Sensitivity heatmap over the $6 \times 6$ grid of TOU ratio $\times$ DR reward scale. Left: net energy cost $f_2$. Right: makespan $C_{\max}$.

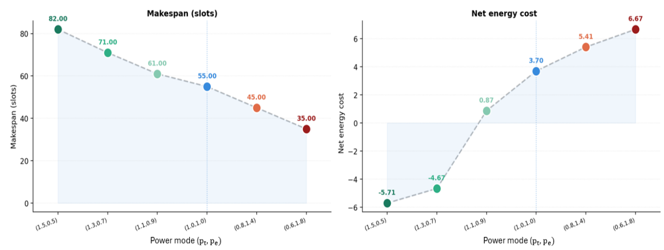


Fig. 4. Impact of the power mode $\mu = (p_t, p_e)$ on makespan (left) and net energy cost (right).

concurrent jobs, leaving a residual grid import at peak price unavoidable. As the TOU ratio increases, this unavoidable fraction becomes proportionally more expensive, overcoming the marginal savings from battery discharge. When DR is active ($\alpha \geq 0.5$), the reward partially offsets this effect, and the TOU ratio influence diminishes as $\alpha$ grows, showing that DR participation mitigates exposure to volatile peak electricity prices.

**Exp-b. DR reward scale impact on energy cost.** Increasing $\alpha$ from 0 to $3\times$ drives the net energy cost from approximately $+4.5$\$ down to $-55.4$\$ across all TOU configurations, a total swing of nearly 60 units. This occurs because a strong reward signal incentivizes the energy management heuristic to aggressively reduce grid imports below the contractual baseline $\overline{C}_t$ during every eligible slot, turning the DR program from a marginal benefit into the primary source of energy savings. This indicates that sufficiently attractive DR incentives can transform energy flexibility into a direct revenue source for manufacturers.

**Exp-a and Exp-b. Makespan decoupling from energy parameters.** The makespan heatmap (Figure 3, right) is nearly constant at $C_{\max} = 57$ across all 36 configurations. A small number of cells achieve $C_{\max} = 55$ or 56, arising from the stochastic nature of the GA rather than any systematic energy-scheduling interaction. This confirms that the lexicographic objective successfully shields production throughput from energy-market variability : regardless of how the energy system is optimized, the GA never delays a job to reduce the energy cost, ensuring that energy-oriented decisions preserve operational performance.

**Exp-c. Power mode impact on schedule duration and energy cost.** Figure 4 shows the effect of varying $\mu = (p_t, p_e)$ across six levels from (1.5, 0.5) to (0.6, 1.8).

Makespan reduces steadily from 82 to 35 slots as $p_t$ decreases, whereas the net energy cost evolves inversely, increasing from $-5.71$ \$ to $+6.67$ \$, a variation of more than 12 \$.

This inversion stems from two compounding effects. Slower modes maintain lower per-slot power consumption, keeping grid imports below the DR contractual baseline $\overline{C}_t$ over a larger number of slots and thereby accumulating DR rewards over a longer horizon, at $(1.5, 0.5)$ and $(1.3, 0.7)$. This accumulation is sufficient to yield negative net costs, effectively turning the facility into a net energy earner. Faster modes, by contrast, concentrate demand into fewer slots at higher instantaneous power ($p_e = 1.8$), saturating the battery and PV buffer and forcing unavoidable grid imports during peak-price periods. The transition point occurs near the baseline $(1.0, 1.0)$, where a modest reduction in operating speed to $(1.1, 0.9)$ already brings the net cost down to $+0.87$\$, indicating a near-break-even point. These results demonstrate that slowing down production extends the DR collection horizon and reduces peak grid stress, highlighting a practical trade-off between throughput and energy profitability.

## VI. Conclusion

An energy-aware genetic algorithm was developed for the flexible flow shop scheduling problem, integrating onsite PV generation, battery storage, TOU pricing, and a demand response reward program, with makespan and net energy cost optimized in lexicographic order. Applied to a 10-job benchmark instance, the approach produces efficient schedules where battery pre-charging during off-peak periods measurably reduces peak-tariff grid imports. The sensitivity analysis shows that the DR reward scale is the dominant cost lever, while the makespan remains stable across all tested configurations, confirming that the lexicographic design effectively decouples production throughput from energy-market variability. Furthermore, the power mode analysis reveals a clear trade-off between schedule duration and energy revenue, where energy-efficient modes extend the demand response horizon and can reduce the net energy cost, whereas energy-intensive modes concentrate demand into fewer slots and increase the net energy cost despite the shorter schedule duration. Future work will extend the framework to dynamic and predictive-reactive scheduling scenarios, and incorporate uncertainty in PV generation forecasts.

## Achnowledgement

This work was supported by the French Environment and Energy Management Agency (ADEME) and CESI.

## References


[1] V. Andrieux, C. Meilhac, and B. Mesqui, "Chiffres clés de l'énergie," ADEME, Tech. Rep., 2023.

[2] X. Xu, Y. Lu, B. Vogel-Heuser, and L. Wang, "Industry 4.0 and industry 5.0—inception, conception and perception," *Journal of Manufacturing Systems*, vol. 61, pp. 530–535, 2021.

[3] M. Sharma, N. Mittal, A. Mishra, and A. Gupta, "Survey of electricity demand forecasting and demand side management techniques in different sectors to identify scope for improvement," *Smart Grids and Sustainable Energy*, vol. 8, no. 2, p. 9, 2023.

[4] K. Bänsch, J. Busse, F. Meisel, J. Rieck, S. Scholz, T. Volling, and M. G. Wichmann, "Energy-aware decision support models in production environments: A systematic literature review," *Computers & Industrial Engineering*, vol. 159, p. 107456, 2021.

[5] S. A. Mansouri, E. Aktas, and U. Besikci, "Green scheduling of a two-machine flowshop: Trade-off between makespan and energy consumption," *European Journal of Operational Research*, vol. 248, no. 3, pp. 772–788, 2016.

[6] H. Öztop, M. F. Tasgetiren, L. Kandiller, D. T. Eliiyi, and L. Gao, "Ensemble of metaheuristics for energy-efficient hybrid flowshops: Makespan versus total energy consumption," *Swarm and Evolutionary Computation*, vol. 54, p. 100660, 2020.

[7] Z. Wei, W. Liao, and L. Zhang, "Hybrid energy-efficient scheduling measures for flexible job-shop problem with variable machining speeds," *Expert Systems with Applications*, vol. 197, p. 116785, 2022.

[8] G. Mouzon, M. B. Yildirim, and J. Twomey, "Operational methods for minimization of energy consumption of manufacturing equipment," *International Journal of Production Research*, vol. 45, no. 18–19, pp. 4247–4271, 2007.

[9] A. Ham, M.-J. Park, and K. M. Kim, "Energy-aware flexible job shop scheduling using mixed integer programming and constraint programming," *Mathematical Problems in Engineering*, vol. 2021, pp. 1–12, 2021.

[10] F. Shrouf, J. Ordieres-Meré, A. García-Sánchez, and M. Ortega-Mier, "Optimizing the production scheduling of a single machine to minimize total energy consumption costs," *Journal of Cleaner Production*, vol. 67, pp. 197–207, 2014.

[11] M. H. Ho, F. Hnaien, and F. Dugardin, "Exact method to optimize the total electricity cost in two-machine permutation flow shop scheduling problem under time-of-use tariff," *Computers & Operations Research*, vol. 144, p. 105788, 2022.

[12] H. Zhang, F. Zhao, K. Fang, and J. W. Sutherland, "Energy-conscious flow shop scheduling under time-of-use electricity tariffs," *CIRP Annals*, vol. 63, no. 1, pp. 37–40, 2014.

[13] M.-J. Park and A. Ham, "Energy-aware flexible job shop scheduling under time-of-use pricing," *International Journal of Production Economics*, vol. 248, p. 108507, 2022.

[14] K. Biel, F. Zhao, J. W. Sutherland, and C. H. Glock, "Flow shop scheduling with grid-integrated onsite wind power using stochastic MILP," *International Journal of Production Research*, vol. 56, no. 5, pp. 2076–2098, 2018.

[15] H. Zhang, J. Cai, K. Fang, F. Zhao, and J. W. Sutherland, "Operational optimization of a grid-connected factory with onsite photovoltaic and battery storage systems," *Applied Energy*, vol. 205, pp. 1538–1547, 2017.

[16] J.-Y. Moon and J. Park, "Smart production scheduling with time-dependent and machine-dependent electricity cost by considering distributed energy resources and energy storage," *International Journal of Production Research*, vol. 52, no. 13, pp. 3922–3939, 2014.

[17] V. Subramanyam, T. Jin, and C. Novoa, "Sizing a renewable microgrid for flow shop manufacturing using climate analytics," *Journal of Cleaner Production*, vol. 252, p. 119829, 2020.

[18] H. Luo, B. Du, G. Q. Huang, H. Chen, and X. Li, "Hybrid flow shop scheduling considering machine electricity consumption cost," *International Journal of Production Economics*, vol. 146, no. 2, pp. 423–439, 2013.

[19] S. Schulz, U. Buscher, and L. Shen, "Multi-objective hybrid flow shop scheduling with variable discrete production speed levels and time-of-use energy prices," *Journal of Business Economics*, vol. 90, pp. 1315–1343, 2020.

[20] Y. Zhai, K. Biel, F. Zhao, and J. W. Sutherland, "Dynamic scheduling of a flow shop with on-site wind generation for energy cost reduction under real time electricity pricing," *CIRP Annals*, vol. 66, no. 1, pp. 41–44, 2017.

[21] J. Mhanna, H. Nouinou, S. Caillard, and D. Baudry, "Energy-aware scheduling in a flexible flow shop using a hybrid constraint programming approach," *International Transactions in Operational Research*, 2026.

[22] Réseau de Transport d'Électricité, "Eco2Mix - Electricity production and consumption in France," 2026, [Online]. Available: https://www.rte-france.com/eco2mix. [Accessed 7 April 2026].